

## Review

# A status review on the thermal stratification modeling methods for Sodium-cooled Fast Reactors

Zeyun Wu<sup>a,\*</sup>, Cihang Lu<sup>a</sup>, Sarah Morgan<sup>a</sup>, Sama Bilbao y Leon<sup>b</sup>, Matthew Bucknor<sup>c</sup>

<sup>a</sup> Department of Mechanical and Nuclear Engineering, Virginia Commonwealth University, Richmond, VA, 23219, USA

<sup>b</sup> OECD Nuclear Energy Agency, 2, rue André Pascal, 75775, Paris, France

<sup>c</sup> Nuclear Science and Engineering Division, Argonne National Laboratory, Lemont, IL, 60439, USA



## ARTICLE INFO

## Keywords:

Thermal stratification  
Sodium-cooled fast reactor  
System code  
CFD  
Coupling methodology

## ABSTRACT

The thermal stratification phenomenon plays a crucial role in the safety of various nuclear systems, including the Gen-III + Light Water Reactors (LWR) and the Gen-IV reactors. The phenomenon is of particular importance for the pool-type Sodium-cooled Fast Reactors (SFRs) because it may cause neutronic and thermal-hydraulic instabilities in the reactor core, or lead to damages of both the reactor vessel and in-vessel components due to the growth of thermal fatigue cracking. More significantly, thermal stratification could impede the establishment of the natural circulation during accidental scenarios and introduce uncertainties to the core safety of SFRs.

Efforts for modeling of the thermal stratification in SFRs have been made for decades to prevent or mitigate the damage caused by the phenomenon. This paper gives a review of the advances that have been made in recent 10 years on the computational modeling methods for thermal stratification phenomenon in SFRs. These methods can be generally drawn into two categories. The first one is the system-level methods which provide fast-running but approximate calculations, and the second one is the CFD methods which provide high-resolution calculations at high computational expense. After introducing the efforts that have been made to improve the one-dimensional (1-D) models, the paper envisioned the possible research directions that could be pursued to enhance the modeling of thermal stratification in the near future.

## 1. Introduction

The thermal stratification phenomenon plays a crucial role in the safety of nuclear reactor systems. This phenomenon could take place in different components of a reactor system. Whenever the fluid entering a volume enclosure has a different temperature to the ambient fluid in the enclosure, a large temperature gradient could then be established. This is generally known as thermal stratification, which will induce significant uncertainties to the safety of the system.

Thermal stratification is of concern in different types of reactor designs, including the Gen-III + Light Water Reactors (LWR) like Economic Simplified Boiling Water Reactor (ESBWR) and AP-1000, as well as the Gen-IV reactor designs like High Temperature Gas Cooled Reactors (HTGRs). In the ESBWR design, the suppression pool is an important passive safety element because it serves as a major heat sink and provides emergency cooling water during accidental scenarios. Because of the large temperature difference between the reactor coolant and the water in the suppression pool, thermal stratification can take place in the

suppression pool, which causes the surface temperature higher than the bulk temperature and in turn increases the vapor pressure and the total containment pressure (Gamble et al., 2001). In the AP-1000 design, the core makeup tank is one of the passive safety systems to remove the decay heat through natural circulation. Thermal stratification could be established in the core makeup tank and impede the natural circulation, which induce uncertainties to the safety of the AP-1000 (IAEA, 2009). In the HTGR design, thermal stratification could also affect the reactor cavity cooling system and impact the decay heat removal from the vessel (IAEA, 2000).

Thermal stratification is of particular concern in the pool-type Sodium-cooled Fast Reactors (SFRs), which is an advanced type reactor this review paper focuses on. The phenomenon could occur in the upper plenum of a pool-type SFR during a down-power transient or a Protected Loss of Flow (PLOF) accident. In such conditions, cooler coolant flows into the lower portion of the upper plenum while the upper portion remains hot, and the stratified layers of sodium coolant with a large vertical temperature gradient is established. As one of the Gen-IV reactor

\* Corresponding author.

E-mail address: [zwu@vcu.edu](mailto:zwu@vcu.edu) (Z. Wu).

designs, the inherent safety of SFR in accidental scenarios relies on capability of natural circulation establishment, which will be impeded by the stratified layers. Moreover, these stratified layers are unstable and could result in low-frequency temperature oscillations of fairly large amplitude (Azarian et al., 1990), which could further cause neutronic and thermal-hydraulic instabilities in the reactor core, or lead to damages of both the reactor vessel and in-vessel components, such as the Upper Instrumentation Structure (UIS), due to the growth of thermal fatigue cracks.

In order to prevent or to mitigate the damage caused by thermal stratification in SFRs, decades-long efforts have been made in different ways to predict this phenomenon with distinct fidelities, including system-level methods, CFD modelings, and the coupling methodologies between the two. Zhao and Peterson (2010) gave a good review of these methodologies till the late 2000s. The current work intends to provide a continued status update on the thermal stratification modeling efforts since early 2010s and introduce outstanding experimental works that are performed in the literature. These experiments provided valuable data for the validation of the modelings. Some work has been included in a preliminary summary published by our group (Morgan et al., 2018) and will be repeated in this paper with more details such that the readers can have a complete overview of the efforts made by the researchers considering modeling thermal stratifications in SFRs.

The rest of the paper is organized as follows: Section 2 introduces outstanding experiments performed and the related analytical findings considering the thermal stratification phenomenon in SFRs. Section 3 presents outstanding system-level methods used for the modeling of the thermal stratification phenomenon in SFRs. Section 4 focuses on outstanding CFD methods for the modeling of the thermal stratification phenomenon in SFRs. Section 5 summarizes the coupling methodologies between system-level methods and CFD methods. Section 6 discusses two latest efforts on the one-dimensional (1-D) thermal stratification modeling, particularly the recent progress made by the reviewers' research group on this subject. Section 7 provides some future perspectives on the modeling of the thermal stratification. The last section (Section 8) offers some conclusions drawn upon this literature review.

## 2. Experimental and analytical researches

Researchers have been conducting experiments mimicking the thermal stratification phenomenon in SFRs and getting prominent analytical findings since several decades ago. These experimental data can be used for the verification and validation of both 1-D system-level method and 3-D CFD method modeling of the thermal stratification phenomenon. Several outstanding experiments and analytical findings associated with the experiments are briefly described in the following section in an order of the year these experiments were performed.

In order to clarify the characteristics of thermal stratification phenomena in Liquid-Metal-cooled Fast Breeder Reactors (LMFBR), Moriya et al. (1987) examined the effects of the Reynolds number ( $Re$ ) and Richardson number ( $Ri$ ) on different thermal stratification phenomena occurred in an LMFBR, including the rising thermal interface, the temperature distribution near the interface, and the internal wave motion. Here  $Re$  expresses the relative importance of inertial and viscous forces on the flow, while  $Ri$  expresses the relative importance of inertial forces and buoyancy forces caused by temperature change within the fluid. They used water as the working fluid in the experiments. Fig. 1 shows the test section of their experiment, which is consisted of a cylindrical tank with a diameter of 80 cm and a height of 90 cm to simulate the hot plenum. Moriya et al. found that the rising speed of the interface increased and the temperature gradient at the interface decreased as the value of  $Re$  increased in the range of  $Re < 10^4$ . On the other hand, the rising speed and the temperature gradient were found to be independent of  $Re$  in the range of  $Re > 10^4$  under a constant  $Ri$  number. Moriya et al. then performed additional experiments in this range to study the effects of  $Ri$ , and found that the rising speed of the interface and the temperature gradient at the interface varied proportionally with  $Ri^{-1/2}$  and  $Ri^{1/2}$ , respectively. Moreover, in the range of  $Re > 10^4$ , large-scale internal waves, which they called internal standing waves, were observed. The internal standing waves were generated in the range  $1 < Ri < 5$ .

In connection with the Phénix and the Superphénix sodium-cooled fast breeder reactors, Vidil et al. (1988) studied the temperature-stratified liquid sodium flow that may occur in SFRs. They used sodium as the working fluid during their experiments. Fig. 2 shows the test section of their experiment, which was named SUPERCANA and consisted of a rectangular channel topped by a rectangular cavity.

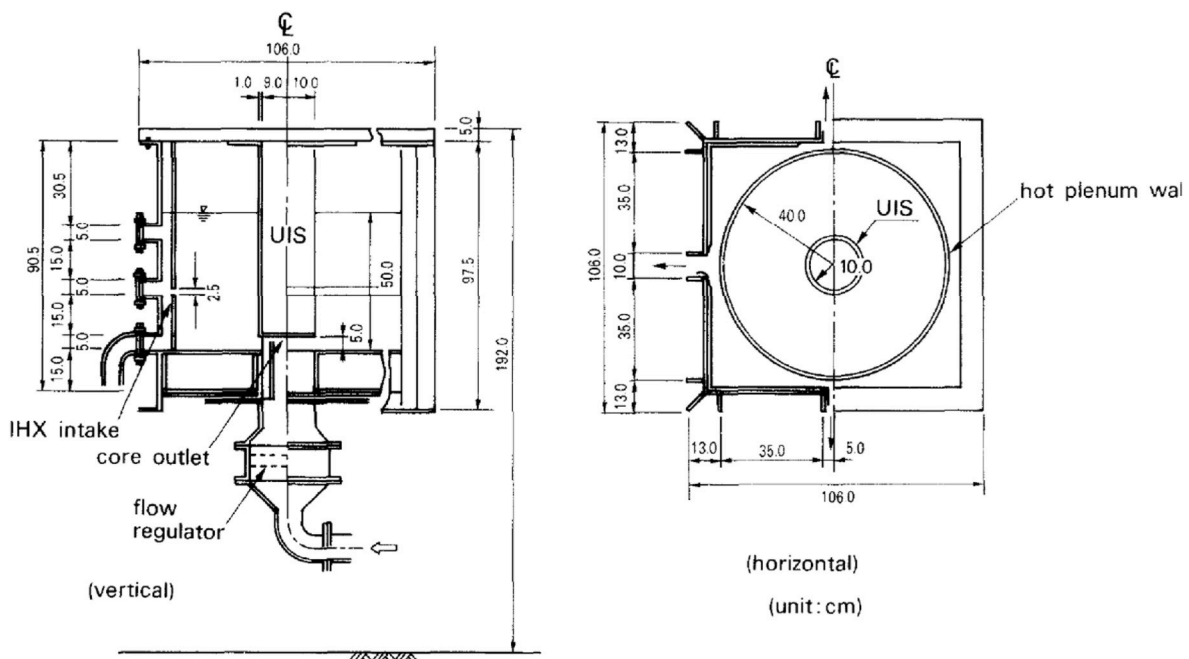


Fig. 1. Schematic of the test section in Moriya et al.'s experiment (Moriya et al., 1987).

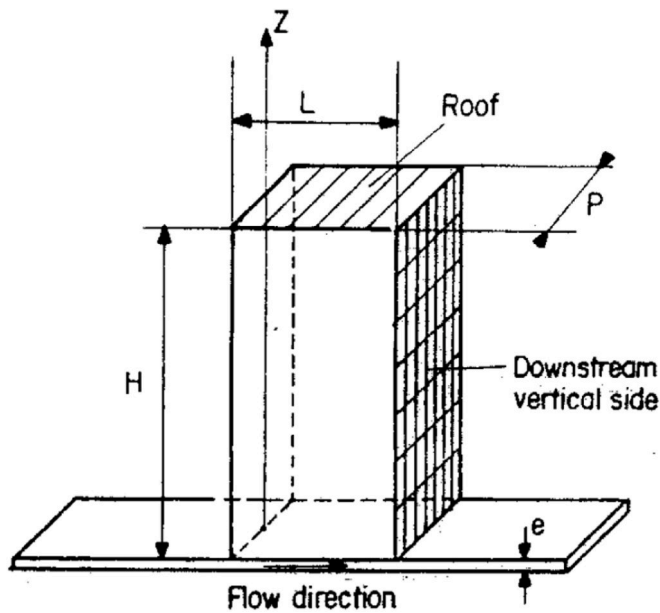


Fig. 2. The SUPERCARVNA cavity used in Vidil et al.'s experiment (Vidil et al., 1988).

The characteristic dimensions of the test section were  $L = 160$  cm,  $H = 320$  cm,  $P = 80$  cm, and  $e = 3$  cm, where  $L$ ,  $H$ ,  $P$  and  $e$  are shown in Fig. 2. The flow forced into the channel would induce a recirculating flow in the cavity. Besides  $Re$  and  $Ri$ , the Peclet number ( $Pe$ ) and the Strouhal number ( $St$ ) were also considered in Vidil et al.'s analysis. Here  $Pe$  expresses the relative effects of convection and diffusion heat transfer on the temperature field, while  $St$  compares the flow convection time with the time constant that is determined based on the initial rate of the thermal transient at the cavity inlet. Vidil et al. proved the possibility to estimate the uncertainties associated with small-scale models.

Ieda et al. (1990) summarized the experimental and analytical results of the thermal stratification tests in the outlet plenum of a loop-type LMFBR. Seven experiments were performed using water or sodium as the working fluid in reactor models with different scales. All the models had the same  $Ri$  and  $Pe$  as the Japanese prototype LMFBR. Fig. 3 shows the experimental configurations of the 1/10 scale model that used sodium as the working fluid. From the experiments, Ieda et al. concluded that  $Ri$  was the dominant factor affecting the occurrence of thermal stratification and the rising rate of the stratification interface. The rising interface rate of sodium was observed to be slower than that of water due to the large difference in  $Pe$ . An oscillatory behavior in the interface was observed when the hotter sodium in the interface was entrained by the colder sodium, proving that the upward motion of the thermal stratification interface was affected by the entrainment process.

Tanaka et al. (1990) conducted experimental studies to examine the applicability of water test results to predict thermal stratification in pool-type LMFBRs. Fig. 4 shows the cylindrical test section used in their experiments. The thermal stratification phenomenon was observed in the test section with both water and sodium used as the working fluid. In the sodium test, the effects of the magnitude of  $Re$  and  $Ri$  on thermal stratification were studied by changing the flow rate and temperature difference between the hot and cold sodium. In the water test,  $Ri$  was fixed and the impact of  $Pe$  was examined. The temperature gradient at the interface was found to be small in the sodium test due to the large thermal conductivity of sodium compared to water. The non-dimensional temperature gradient obtained from the water test result was found rather close to real plant values, while the small-scale test result yielded a much smaller temperature gradient.

Muramatsu and Ninokata (1994) performed experiments to acquire experimental data to investigate the impact of the turbulence model

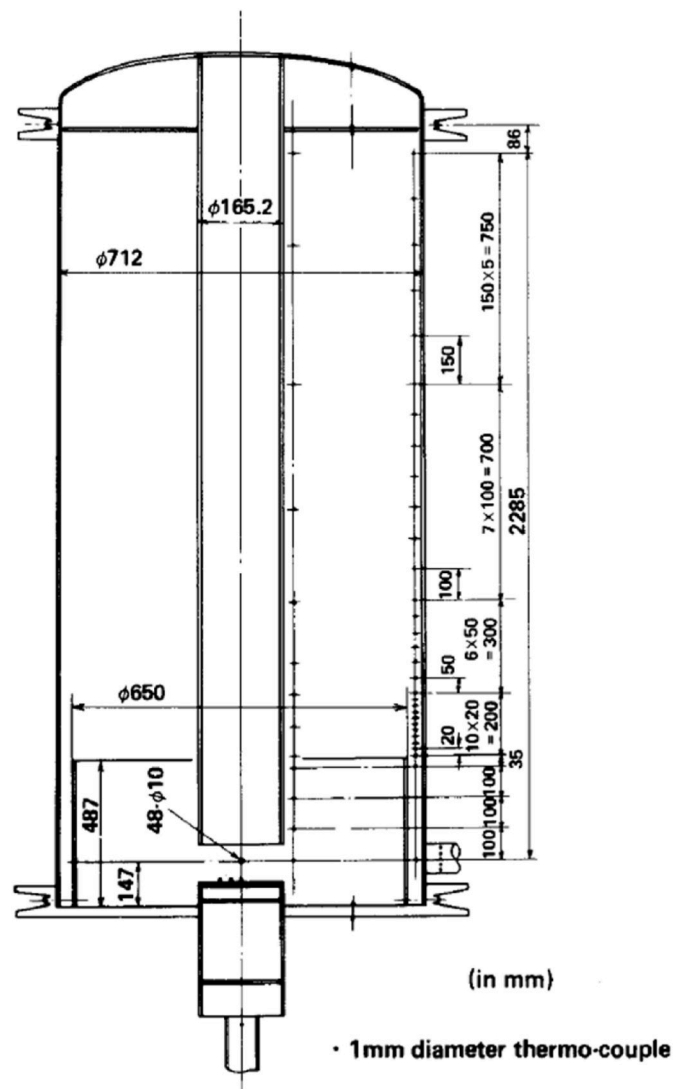


Fig. 3. Schematic of the test section in Ieda et al.'s experiment. (Ieda et al., 1990).

used on their CFD predictions of the thermal stratification. The experiment was performed in a 1/10 scale model of the Japanese prototype LMFBR, as shown in Fig. 5, using sodium as working fluid. The CFD simulation results of these experiments will be discussed in Section 3.

A turbine trip test at 40% of nominal electrical power was performed in the Japanese MONJU sodium-cooled fast breeder reactor in 1995, and thermal stratification interfaces were observed due to the flow coast-down after the turbine trip in the upper plenum of the MONJU reactor (Doi and Muramatsu, 1997). During the transient, thermocouples were used for the measurement of the axial temperature distribution in the upper plenum of MONJU reactor, which consisted of the upper instrument structure (UIS), the inner barrel, and the core barrel with three outlet pipes, as shown in Fig. 6 (Shibahara et al., 2013). The experimental data obtained from this transient was widely used for the validation of different system-level codes and CFD codes, as introduced later in Sections 3 and 4.

In order to evaluate the thermal stratification phenomena in the upper plenum of the reactor vessel in an innovative sodium-cooled fast reactor (JSFR), Kimura et al. (2010) performed experiments in a 1/10 scale model of the JSFR, as shown in Fig. 7, using water as the working fluid. In this study, Kimura et al. examined the effects of thermal stratification due to the thermal loss to the reactor vessel wall caused by the temperature gradient and fluctuation.

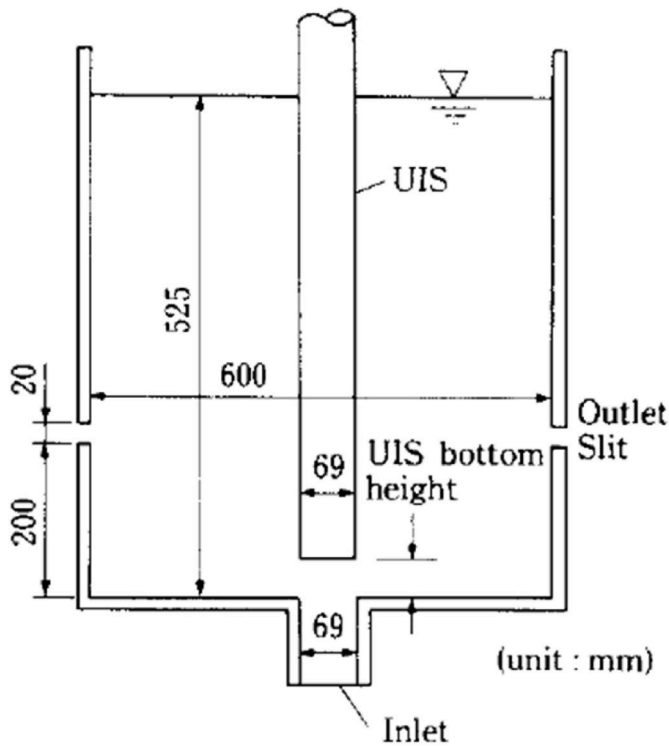


Fig. 4. Schematic of the test section in Tanaka et al.'s experiment. (Tanaka et al., 1990).

Most recently, Ward et al. (2019) performed experiments in a liquid gallium pool, aiming to investigate the thermal stratification transitions where flow fluctuations caused by the impinging jets were able to overcome the restoring buoyant forces. They used gallium as the working fluid, and Fig. 8 shows the test section of their experiment. Schneider et al. (2019) performed experiments to provide experimental data to validate system-level 1-D models for the thermal stratification. Fig. 9 shows the test section used in Schneider et al.'s experiment. The cylindrical test section had a height of 128 cm and a diameter of 31 cm, and the working fluid used in the experiment was sodium. As indicated in Fig. 9, twelve thermocouples were installed in the test section at six different axial levels for convenient temperature measurements. Two outlets at different levels were designed to examine the thermal stratification. However, only the high outlet has really been used to generate experimental data. The temperature measurements, obtained from the eight thermocouples located lower than the high outlet, were used for the validation of the newly developed 1-D thermal stratification models (Lu et al., 2019, 2020), which will be further discussed in Section 6. Table 1 summarizes all the experimental works discussed in this section.

### 3. System-level methods

Major system-level codes currently employed in the U.S. for the analysis of both real and postulated transients in LWRs, such as TRAC (U.S. NRC, 2001) and MELCOR (U.S. NRC, 2005), either have no models or only 0-D models for the prediction of the thermal stratification. Due to the lack of reliable thermal stratification models, the accuracy of these codes is limited when thermal stratification phenomenon is important in the nuclear system. Several recent verification and validation efforts of the existing system codes on the modeling of thermal stratification are summarized in this section.

Bandini et al. (2015) discussed the calculations of three transients involving thermal stratification phenomena with RELAP5/MOD3.3 (ISL, 2003) and TRACE, including a start-up of forced circulation, a loss-of-heat-sink transient, and a loss-of-pump transient. Their

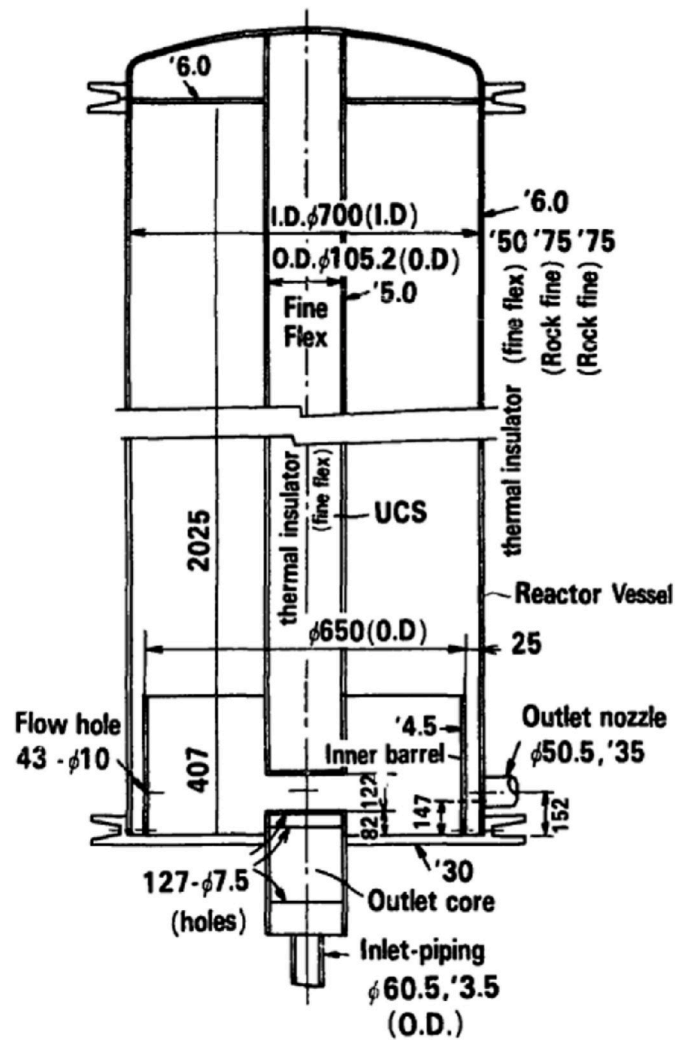


Fig. 5. Schematic of the test section in Muramatsu and Ninokata's experiment. (Muramatsu and Ninokata, 1994).

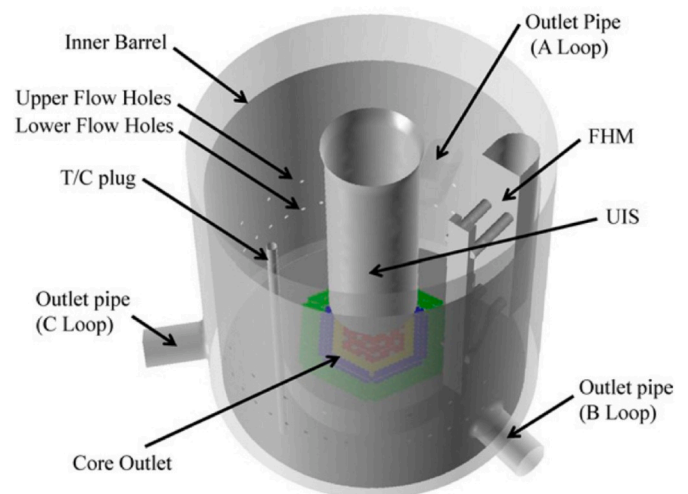


Fig. 6. Schematic of the upper plenum of the MONJU reactor (Shibahara et al., 2013).

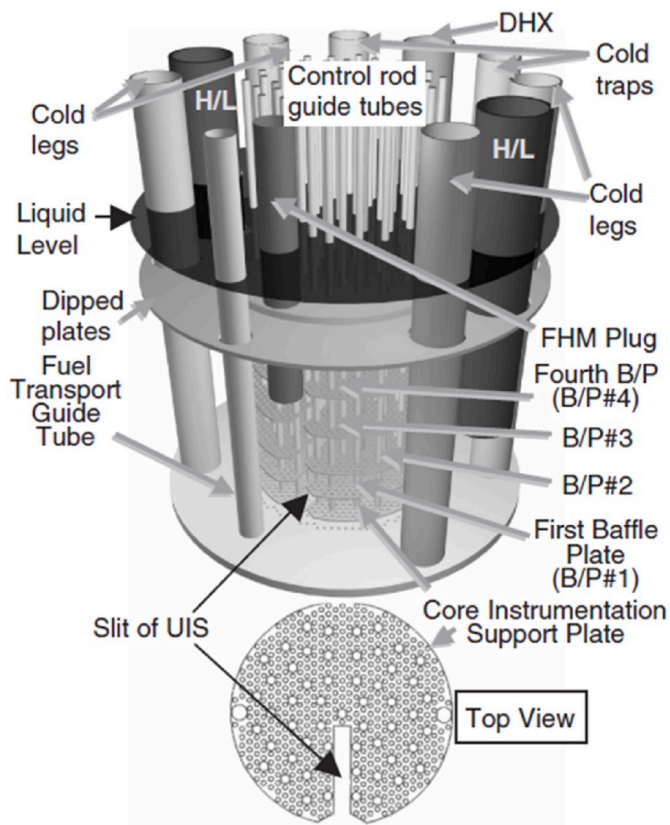


Fig. 7. Schematic of the test section in Kimura et al.'s experiment (Kimura et al., 2010).

RELAP5/MOD3.3 models were validated with several transients performed on the TALL facility (Ma et al., 2007), which was operated at KTH Royal Institute of Technology in Stockholm from 2003 to 2009. TALL facility used liquid lead bismuth eutectic (LBE) as the working fluid. For additional validations, RELAP5/MOD3.3 was also used to simulate the Decay Heat Removal (DHR) experiments performed in the CIRCE test facility, which also uses LBE as working fluid, and was designed and realized by the Italian agency ENEA to support the heavy liquid metal technology for nuclear fission plants (Bandini et al., 2015).

More recently, improvements have been made to RELAP5-3D (INL, 2015), the latest version of the RELAP5 series, such that the multi-dimensional components can be used for the modeling of multi-dimensional flow behaviors, including thermal stratification. Narcisi et al. (2019) assessed the performance of RELAP5-3D with the latest improvements. Through comparisons conducted between calculation results and experimental data obtained from the CIRCE test facility, they proved that RELAP5-3D is able to provide reasonable prediction for thermal stratification in liquid-metal-cooled pool-type reactors by modelling the pool with multiple channels, with cross junctions, or with a multi-dimensional component.

The SAS4A/SASSYS-1 fast reactor safety analysis code (Fanning et al., 2017), developed by Argonne National Laboratory (ANL), is one of the major SFR system analysis codes. For thermal stratification modeling, SAS4A/SASSYS-1 only uses lumped-volume-based 0-D models at different mixing stages, and thus can only provide approximate results. The stratified volume model currently used in the thermal-hydraulic solver PRIMAR-4 of SAS4A/SASSYS-1 was derived from the older PLENUM-2A model by Howard and Lorenz (Fanning et al., 2015). The newer model is now able to handle up transients, down transients, and horizontal discharges. The newer model considers three regions and five stages, which improves the previous two region model. Fig. 10 shows the various stages and cases considered in the current

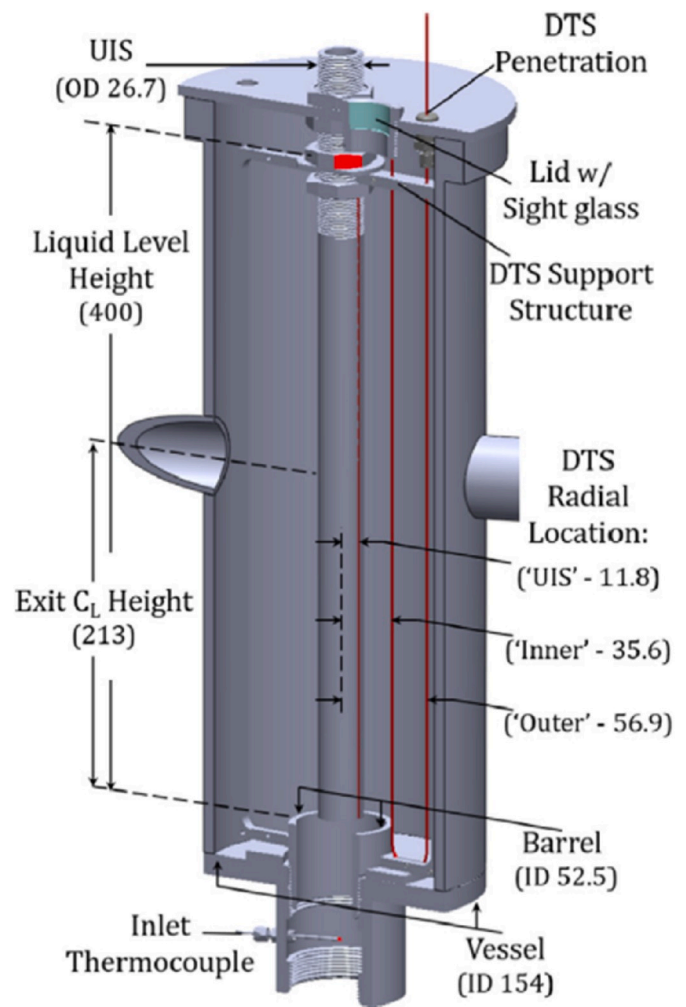


Fig. 8. The Gallium Thermal-hydraulic Experiment (GaTE) test section in Ward et al.'s experiment (Ward et al., 2019).

SAS4A/SASSYS-1 model. Fanning and Thomas (2010) simulated the Loss of Flow (LOF) transient in the Toshiba 4S micro sodium reactor design using SAS4A/SASSYS-1, and assessed the impact of coupling SAS4A/SASSYS-1 with CFD codes.

Pialla et al. (2015) provides an excellent review of three European system-level codes, including DYN2B, CATHARE, and ATHLET. For completeness, important features of these three codes on the modeling of the thermal stratification in SFRs are reiterated as follows.

DYN2B is a system code dedicated for the pool-type SFR safety analyses (Note SYFRA, 1993). It was developed by NOVATOME (A division of Framatome, the company that produced fuel for Phénix and Superphénix) and French Commission for Atomic Energy (CEA) in the 1980s. DYN2B is essentially the reference thermal-hydraulic system code in France for Phénix and Superphénix thermal hydraulics safety studies. DYN2B uses 1-D models for the core, heat exchangers, steam-generators and pipes, and 0-D models based on  $Ri$  for the hot and cold pools to take into account of the thermal stratification conditions (Pialla et al., 2015).

CATHARE is the reference thermal-hydraulic system code in France for the pressurized water reactor (PWR) safety analyses. It has been developed in collaboration of CEA, Electricity of France (EDF), French Institute for Radiological Protection and Nuclear Safety (IRSN), and AREVA-NP (now Framatome) for more than 30 years. Under the umbrella of the Generation IV, intensive developments have been accomplished to extend the modeling capabilities of CATHARE to other fluids for advanced reactor analysis. Calculations for SFRs are now enabled in the industrial release version of CATHARE (Geffraye et al., 2009), which

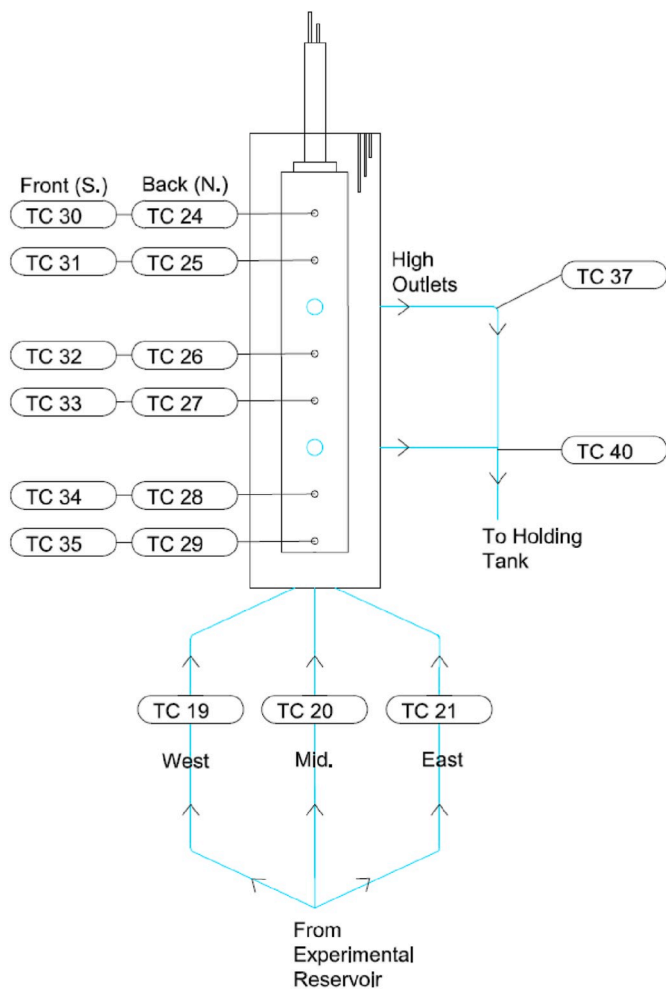


Fig. 9. Schematic of the test section in Schneider et al.'s experiment (Schneider et al., 2019).

Table 1  
Experimental and analytical works considering the thermal stratification in SFRs.

Authors	Year	Working fluid	Dimensionless numbers considered
Moriya et al.	1987	Water	$Re, Ri$
Vidil et al.	1988	Sodium	$Re, Ri, Pe, St$
Ieda et al.	1990	Water and Sodium	$Re, Ri, Pe$
Tanka et al.	1990	Water and Sodium	$Re, Ri, Pe$
Muramatsu and Ninokata	1994	Sodium	-
Kimura et al.	2010	Water	-
Ward et al.	2019	Gallium	$Re, Ri, Pr$
Schneider et al.	2019	Sodium	-

has been used to simulate the thermal-hydraulic Natural Convection Test (NCT) conducted in Phénix. These calculation results were compared to those obtained from coupled TRIO\_U (an CFD code discussed in the next section) and CATHARE to justify the thermal stratification modeling capability in CATHARE (Bandini et al., 2015).

ATHLET is a thermal-hydraulic system code developed by German Society for Plant and Reactor Safety (GRS). Because it was originally developed for transient analyses for LWRs, its physical modules, including the thermo-physical properties package, heat transfer

correlations, etc., are water oriented (Lerchel and Austregesilo, 2006). The modeling capability of ATHLET was extended to SFRs by implementing various sodium thermo-physical and transport properties and dedicated heat transfer correlations (Zhou et al., 2013). Zhou et al. performed calculations of the Phénix NCT using the modified ATHLET code and proved its good applicability to the sodium-cooled reactor systems.

Super-COPD, developed by Japan Atomic Energy Agency (JAEA), is an improved version of the MONJU plant dynamics analysis code COPD, which divides the flow network models of the main components and control systems into simple calculation modules. Yamada et al. (2014) validated Super-COPD using the experimental data from the MONJU turbine trip test. Watanabe et al. (2015) and Oyama et al. (2016) also validated Super-COPD using the experimental data from a sodium loop test performed at the Plant Dynamic Test Loop (PLANDTL) of O-arai Engineering Center of JAEA. The purpose of this test was to investigate the decay heat removal capability through natural circulation (Kamide et al., 2011).

MARS-LMR, developed by the Korea Atomic Energy Research Institute (KAERI), is a thermal hydraulics system code specifically for transient analyses in SFRs. MARS-LMR can use either 1-D or multi-dimensional approaches to model large volumes such as the cold pool and the hot pool. Jeong et al. simulated the Phénix end-of-life asymmetric test using MARS-LMR (Jeong et al., 2015). By comparing the calculations results with experimental data, they found the 1-D approach is inadequate to describe the complicated mixing phenomena in the pools of an SFR. Choi and Ha (2016) also simulated EBR-II Shutdown Heat Removal Test (SHRT) – 17 benchmark problem with MARS-LMR. EBR-II SHRT-17 was the most severe protected loss of flow test performed during the SHRT program, which demonstrated the effectiveness of natural circulation in cooling the reactor (Sumner and Moisseytsev, 2015). During the SHRT-17 test, EBR-II completely lost all pumping power while operating at full power and flow, followed with a SCRAM. Choi and Ha (2016) EBR-II SHRT-17 simulation indicated that the results calculated by MARS-LMR were overall in good agreement with the experimental data.

SSC-K (Kwon et al., 2000) is another system code developed in Korea for the analysis of the pool-type Korea Advanced LIquid METal Reactor (KALIMER) design. SSC-K is the daughter code of SSC-L, which was originally developed at Brookhaven National Laboratory for the analysis of a loop-type liquid metal reactor. The development of SSC-K from SSC-L enhanced its applicability on pool-type reactors. In SSC-K, the thermal stratification phenomenon in the hot pool is solved by a two-zone model during very slow transitions or steady state conditions, as shown in Fig. 11 (Chang et al., 2002). Otherwise, a two-dimensional pool model can be used as an alternative to calculate the coolant temperature and velocity profiles in the hot pool (Lee et al., 2000).

The BMIX++ (Berkeley mechanistic MIXing code in C++) was developed at UC Berkeley based on Peterson's pioneering work on the thermal stratification (Peterson, 1994). Peterson performed a scaling analysis of a large volume enclosure and identified the non-dimensional parameters governing the onset and the breakdown of thermal stratification. He also found that once thermal stratification is established in the ambient fluid, the temperature and species distributions can be described by 1-D differential equations integrated with standard jet models. Based on these findings, BMIX++ calculates the mixing and stratification in a large stratified enclosure through two parts: (1) using 1-D Lagrangian method to track movable control volumes and model the ambient volume; (2) using 1-D integral methods or analytical methods to model different types of jets. These two parts are coupled through entrainment and discharge processes (Niu et al., 2007). BMIX++ was successfully applied to simulate the thermal stratification in the buffer pool of an Advanced High Temperature Reactor (AHTR) design during Loss of Forced Cooling (LOFC) transients (Zhao and Peterson, 2007, 2009). BMIX++ is not a production level system code, but it can be coupled with other system analysis codes to perform the whole plant

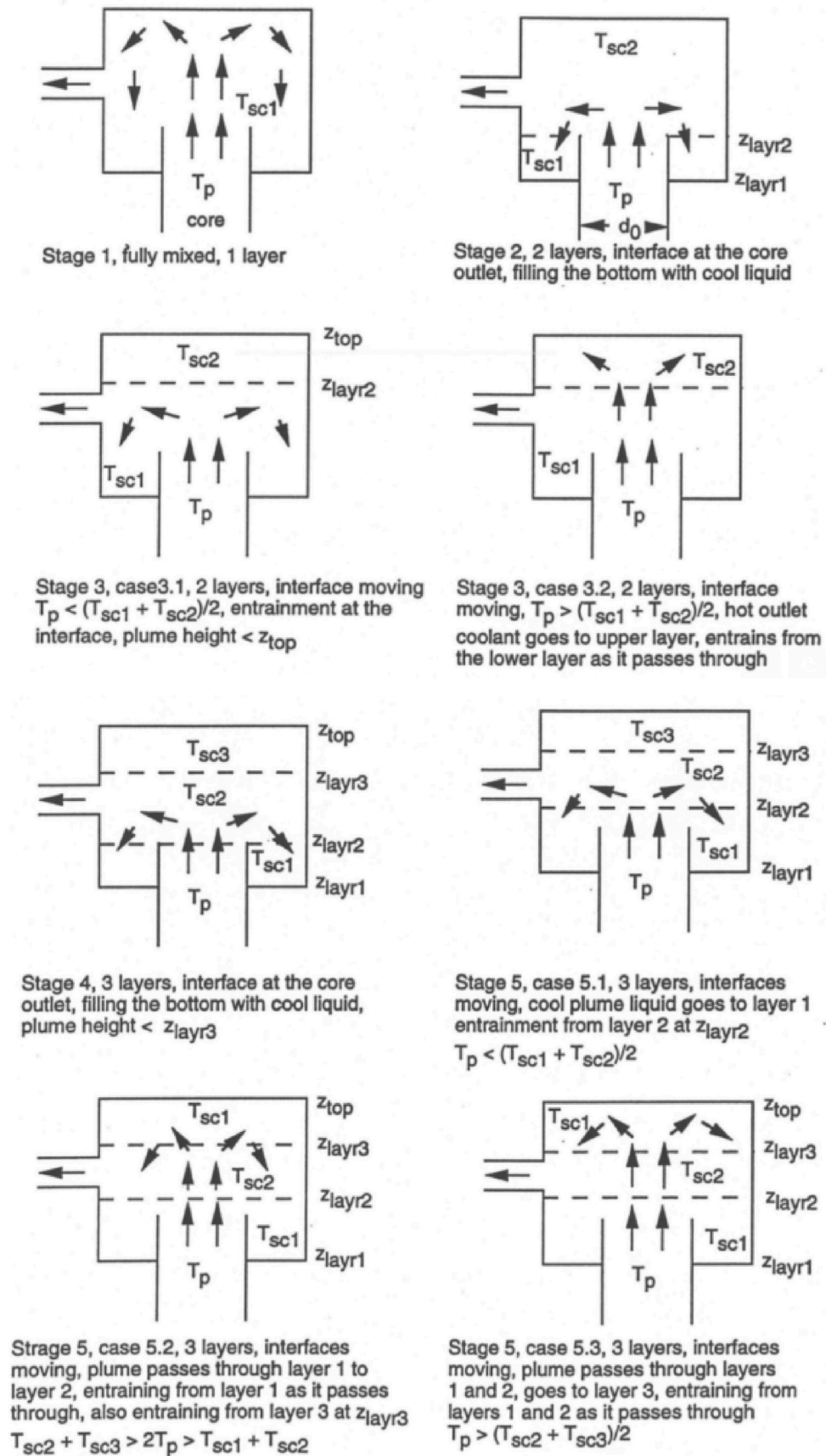


Fig. 10. Stratified volume stages in SAS4A/SASSYS-1 (Fanning et al., 2017).

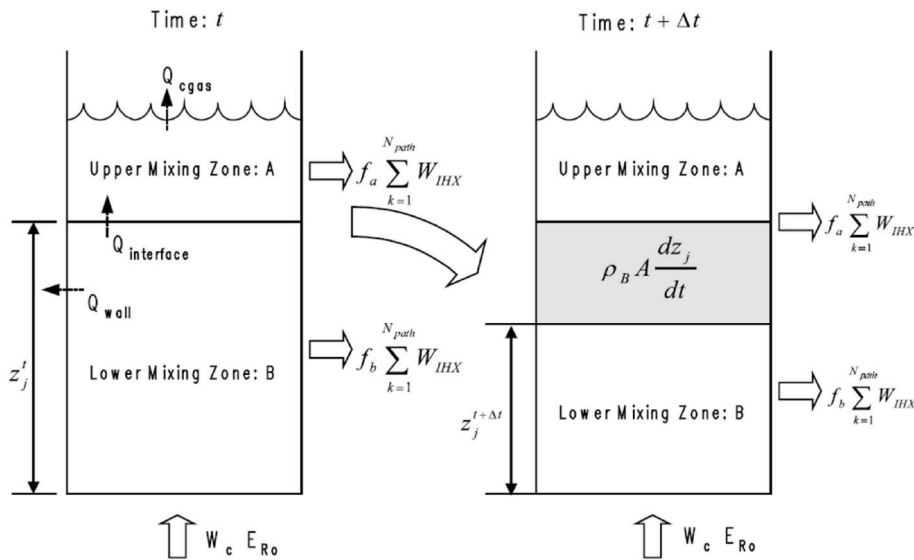


Fig. 11. The two mixing zone model for the hot pool in SSC-K (Chang et al., 2002).

analyses.

THACS (the Transient Thermal-Hydraulic Code for Analysis of Sodium Cooled Fast Reactor) is a system-level code developed by XJTU (Xi'an Jiao Tong University) for the analysis of accidents in SFRs. Yue et al. (2015) evaluated the performance of THACS by simulating EBR-II SHRT-17 and SHRT-45R, which was a loss-of-primary-flow transient without SCRAM. A three-layer-pool model was employed in their calculation in order to correctly capture the thermal stratification phenomenon. Reasonable predictions were made by THACS, but discrepancies between predicted results and measured data were observed.

As a short summary to this section, the system-level codes can provide consistent predictions of the nominal states with the experimental data. However, they more or less encounter problems to properly calculate some sharp evolutions of temperature during the transients due to some complex 3-D effects or buoyancy effects of the phenomena, especially at the onset of natural convection (Bandini et al., 2015).

Table 2 summarized the system-level codes discussed in this section.

#### 4. CFD methods

With the improving computation power, the computational fluid dynamics (CFD) modeling of the thermal stratification phenomenon has

**Table 2**  
Works considering modeling thermal stratification in SFRs with system-level codes.

Authors	Year	Codes employed	Experimental data used for validation
Bandini et al.	2015	RELAP5/MOD3.3	CIRCE DHR experiments
Narcisi et al.	2019	RELAP5-3D	CIRCE experiments
Fanning and Thomas	2010	SAS4A/SASSYS-1	Toshiba 4S LOF transient
Pialla et al.	2015	DYN2B	–
Bandini et al.	2015	CATHARE	Phénix NCT test
Zhou et al.	2013	ATHLET	Phénix NCT test
Yamada et al.	2014	Super-COPD	MONJU turbine trip test
Watanabe et al.	2015	Super-COPD	PLANDTL decay heat removal test
Oyama et al.	2016	MARS-LMR	Phénix asymmetric test
Jeong et al.	2015	MARS-LMR	EBR-II SHRT-17
Choi and Ha	2016	MARS-LMR	–
Kwon et al.	2000	SSC-K	–
Zhao and Peterson	2007	BMIX++	–
	2009		
Yue et al.	2015	THACS	EBR-II SHRT-17, SHRT-45R

been proven feasible. Many CFD codes have been used and compared to each other with different models to find a reliable analysis method for thermal stratification phenomena. Much work on CFD modeling has been involved significant verification and validation (V&V) efforts on these codes. This section summarized several recent CFD modeling works on this regard.

Muramatsu and Ninokata (1994) studied the impact of the turbulence model used on the resultant CFD prediction for the thermal stratification. The JAEA CFD code AQUA (Maekawa et al., 1991) was used for the numerical calculation. After comparing the CFD calculations with the experimental data, the authors found the choice of turbulence model is vital important for a proper prediction of thermal stratification in a sodium system.

Ohno et al. (2011) investigate the applicability of commercial CFD codes on evaluating the thermal stratification behavior in the upper plenum of an SFR. The authors first used AQUA to study the impact of the spatial mesh distribution, and then used the commercial CFD codes Fluent and STAR-CD to simulate the sodium thermal stratification experiments performed by Ieda et al. (1990) with different turbulence models. After comparing the CFD simulations results with the experimental data, the authors concluded that both commercial codes were applicable to evaluate the basic behaviors of thermal stratification. The turbulence models used did not remarkably impact the numerical simulation results, whereas the spatial mesh arrangement around the thermal stratification interface in the gravitational direction had shown more significant impact.

The International Atomic Energy Agency (IAEA) coordinated a research project named “Benchmark Analysis of Sodium Natural Convection in the Upper Plenum of the MONJU Reactor Vessel” aiming to validate multi-dimensional CFD and turbulence models for predicting thermal stratification in the upper plenum of a fast reactor. The project was carried out between 2008 and 2012. Detailed geometrical data and time-dependent inlet conditions of the flow rate and temperature for the transient analysis of the MONJU trip test were provided by JAEA to the participating research organizations. Eight participants, including ANL (USA), CEA (France), CIAE (China), IGCAR (India), IPPE (Russia), JAEA (Japan), KAERI (Korea), and University of Fukui (Japan), were asked to perform calculations for the same problem with different numerical methods or turbulence models (Ohira et al., 2013). Sakamoto et al. (2010) simulated the transient with Fluent, and found that the resultant thermal stratification interface was affected by the mesh arrangement of the flow holes. Sofu (2012) used both commercial CFD codes STAR-CD and STAR-CCM+ to examine the 1/6 upper plenum in the MONJU trip

test, and found that the average temperature of the coolant through the outlet nozzle decreased early while the upper plenum remained hotter for much longer because the MONJU design provided alternative flow paths that bypassed the thermally stratified upper plenum region. [Shibahara et al. \(2013\)](#) used Fluent to simulate the transient and found that the thermal stratification interface was influenced by the flow pattern in the upper plenum of MONJU. Their numerical results were consistent with experimental data until about 240 s, after which point the interface ascended faster in the 3-D simulations than that of experimental data. [Choi et al. \(2013\)](#) used the commercial CFD code CFX to simulate both the steady state and the transient of the MONJU turbine trip test. The fluid temperature was predicted accurately in the initial rapid coast-down period before 300 s elapsed time, while a faster thermal mixing was obtained numerically than that shown in the experimental data after 600 s elapsed time. This discrepancy was explained by the shortcomings of the thermal turbulence models available in the CFX code for a natural convection flow with thermal stratification. [Mochizuki and Yao \(2014\)](#) also pointed out the bypass flow holes may cause modeling problems. They used Fluent to show that the flow rate through the bypass flow holes had a definite impact on the thermal stratification behavior. They found the total energy transferred into the upper plenum was insufficient for modeling when the boundary conditions specified in the IAEA benchmark were used.

[Wang et al. \(2018\)](#) developed a novel 2-D CFD analysis program under cylindrical coordinate to predict the in-vessel thermal stratification in SFRs, where complex structures were addressed by employing non-orthogonal block-structured grids. Wang et al. validated their program against experiments performed in two distinct facilities, including the experiments performed by [Ieda et al. \(1990\)](#) and the turbine trip test performed in the MONJU reactor, which were introduced in [Section 2](#). The computational expense was about 3.5 core-hours and 35.5 core-hours for two transients with physical times of 500 s and 3600 s, respectively. Through the validation process, Wang et al.'s program was demonstrated to have the ability to reasonably reproduce the overall behaviors of the thermal stratification in SFRs.

More recently, CFD calculations were conducted considering the Advanced Burner Test Reactor (ABTR), which is a pre-conceptual 250 MWt SFR designed to transmute the spent nuclear fuel of the LWRs. [Munkhzul and Thomas \(2014\)](#) used STAR-CCM+ to examine the impact of thermal stratification on the start of natural circulation during a transient for the ABTR design. [Ward et al. \(2018\)](#) used CFX calculations to confirm that their scaled-down experimental facility could accurately represent thermal stratification and mixing in the ABTR prototype under all flow conditions. [Zwijsen et al. \(2019\)](#) used both Fluent and STAR-CCM+ to simulate the transients performed in the CIRCE facility, and obtained good agreement between the calculation and the experimental data. [Lu et al. \(2020\)](#) performed CFD calculations with STAR-CCM+ to inform the design of their experimental facility and to provide CFD calculation for the validation of their 1-D thermal stratification model.

As a short summary to the CFD computational efforts described above, CFD models are able to predict the thermal stratification phenomenon in the SFRs when fine grid is used to resolve thin substructures. However, due to the high computational cost generally observed, the CFD modeling is not a suitable computation means when a large number of reactor transient of calculations are needed for core safety analysis. [Table 3](#) summarizes the CFD works discussed in this section.

## 5. Coupling system-level and CFD methods

CFD method generally cannot be used alone for whole plant transient analyses because it may require unacceptable high computational cost. To obtain efficient and reliable computational results, a compromised strategy has been explored by several methodologies to couple system-level codes with CFD codes for the whole plant transient analyses. In these methods, the regions of 3-D interest are modeled by the CFD codes

**Table 3**  
CFD works considering the modeling of thermal stratification in SFRs.

Authors	Year	CFD codes employed	Experimental data for validation
Muramatsu and Ninokata	1994	AQUA	The same work
Sakamoto et al.	2010	Fluent	MONJU turbine trip test
Ohno et al.	2011	AQUA, STAR-CD, and Fluent	<a href="#">Ieda et al. (1990)</a>
Sofu	2012	STAR-CD and STAR-CCM+	MONJU turbine trip test
Shibahara et al.	2013	Fluent	MONJU turbine trip test
Choi et al.	2013	CFX	MONJU turbine trip test
Mochizuki and Yao	2014	Fluent	MONJU turbine trip test
Munkhzul and Thomas	2014	STAR-CCM+	–
Ward et al.	2018	CFX	–
Wang et al.	2018	Program developed in the same work	<a href="#">Ieda et al. (1990)</a> MONJU turbine trip test
Zwijsen et al.	2019	Fluent and STAR-CCM+	The same work
Lu et al.	2020	STAR-CCM+	The same work

while the rest of the reactor circuit is modeled by the system-level codes. Feedbacks are provided mutually between the system-level codes and the CFD codes when the whole plant analysis is performed. This section summarized several recent works using the system code and CFD codes coupling approach to simulate the thermal stratification phenomena.

[Fanning and Thomas \(2010\)](#) simulated an LOF transient in the Toshiba 4S micro sodium reactor design by coupling SAS4A/SASSYS-1 with STAR-CD. Their earlier attempts to couple these two codes employed only a unidirectional data transfer from SAS4A/SASSYS-1 to STAR-CD, with no feedback from STAR-CD to SAS4A/SASSYS-1. They found the SAS4A/SASSYS-1 calculation results were identical to the uncoupled calculations. In their updated work, Fanning and Thomas improved the evaluation of the influence of thermal stratification in the outlet plenum by providing the STAR-CD prediction of the core and internal heat exchanger (IHX) inlet temperatures and pressures back to SAS4A/SASSYS-1. Comparisons of the results proved the indispensability of the two-way communications between the coupled models in order to get an accurate prediction of the LOF transient. This work demonstrated that with a proper coupling approach, a high-fidelity CFD tool can be used to resolve the important flow and temperature distributions in a reactor outlet plenum while maintaining the whole plant safety analysis capability of a system analysis code. However, their coupled simulations on a quad-core machine required approximately 39 h on the LOF transient calculations.

[Thomas et al. \(2012\)](#) simulated the EBR-II SHRT-17 problem by coupling SAS4A/SASSYS-1 with STAR-CCM+. In their calculation, SAS4A/SASSYS-1 was used to model the primary coolant system of the reactor, and STAR-CCM+ was used to model the cold pool to replace the control volume in SAS4A/SASSYS-1. SAS4A/SASSYS-1 provided STAR-CCM+ with the flow rate and the temperature distribution at the plenum inlet boundary, while STAR-CCM+ provided SAS4A/SASSYS-1 with the gravity head that reflected the temperature distribution in the plenum. During the coupled simulation, SAS4A/SASSYS-1 and STAR-CCM+ exchanged information at the beginning and end of each time step of SAS4A/SASSYS-1. The coupled simulation showed good agreement with the experimental data, yet required about 160 h of calculation time on a workstation with 32 cores to complete the whole transient calculations.

[Pialla et al. \(2015\)](#) analyzed the Phénix NCT transient with two different coupling methodologies. The Phénix NCT was performed in the Phénix sodium-cooled fast reactor before its decommission. Starting from a reduced power state of 120 MWt, the NCT consisted of a loss of the heat sink combined with a reactor SCRAM and a primary pumps trip leading to stabilized natural circulation in the primary sodium system. Pialla et al. first investigated the coupling between CATHARE and TRIO\_U ([Tenchine et al., 2012](#)), an CFD code developed by CEA. Under

this coupling scheme, the hot collector, cold collector and upper-core structure of the reactor were modeled with TRIO\_U, while the pumps and the reactor core were modeled with CATHARE. During the NCT transient calculation, data were exchanged at every time step: CATHARE computed a time step and gave mass flow rate and temperature boundary conditions to TRIO\_U, then TRIO\_U computed a time step and gave momentum and enthalpy feedbacks to CATHARE. Their first coupled calculation was finished in 96 h using 200 cores. Their second coupling calculation was developed between ATHLET and the Open Field Operation and Manipulation CFD Toolbox (OpenFOAM), which is an open-source CFD software package. Under this coupling scheme, the hot plenum was modeled with OpenFOAM, while the rest of the primary circuit was modeled with ATHLET. The OpenFOAM calculation strongly depended on the initial calculation results of ATHLET because the values of mass flow rate, temperatures and pressure must be provided by ATHLET to OpenFOAM as boundary conditions. In the coupling approach, neither ATHLET nor OpenFOAM could be considered as the master code to handle time steps individually, and the full transient was iterated between the two codes. The iterations were handled by a python program and considered converged when the exchanged values showing non-significant changes at boundaries compared previous iteration results. The second coupled calculation was finished in 192 h by using 9 cores.

Bandini et al. (2015) simulated the transients performed in TALL-3D with two different coupling methodologies. The TALL-3D facility is a LBE loop developed to provide experimental data for the validation of coupled system-level and CFD codes. Bandini et al. first investigated the coupling method between RELAP5/MOD3.3 and Star-CCM+. Under this coupling method, the 3D test section and the inlet and outlet pipes were modeled with Star-CCM+, while the rest of the primary loop, the secondary loop, and the heat exchanger were modeled by RELAP5/MOD3.3. The coupling between the two codes was managed by a Java program. During the transient, the two codes worked in parallel with information exchanged at every coupling time step. At a coupling time step, Star-CCM+ ran first with time-extrapolated and cross-section-averaged inlet mass flow and temperature boundary conditions. Thereafter, RELAP5/MOD3.3 iteratively computed the energy source/sink needed to match the temperatures in both solutions. Their second coupling was performed between ATHLET and CFX. In this coupling, the test section was modeled by CFX, while the rest of the whole experimental facility was modeled by ATHLET. The calculation results were compared to those obtained by stand-alone ATHLET. As expected, the detailed results in the complex 3-D regions differed when adding the 3-D CFD analysis. However, it was observed that the overall predictions for the entire transient progression in the facility were very similar.

As can be seen, various system-level and CFD coupling methods have been realized to achieve calculation results of the transients to have good agreement with the experimental data. The use of the coupling was proven indispensable for an accurate prediction of the transients.

**Table 4**

Coupled works considering the modeling of thermal stratification in liquid-metal-cooled systems.

Authors	Year	Coupled codes	System simulated	Computational expense
Fanning and Thomas	2010	SAS4A/SASSYS-1 with STAR-CD	Toshiba 4S	4 cores, 39 h
Thomas et al.	2012	SAS4A/SASSYS-1 with STAR-CCM+	EBR-II	32 cores, 160 h
Pialla et al.	2015	CATHARE with TRIO_U ATHLET with OpenFOAM	Phénix	200 cores, 96 h 9 cores, 192 h
Bandini et al.	2015	RELAP5 with Star-CCM+ ATHLET with CFX	TALL-3D	– –

However, because of the CFD calculations involved, current coupling methods are still extremely computational expensive and time consuming (Pialla et al., 2015; Bandini et al., 2015). Table 4 summarizes the system-level-CFD coupled works discussed in this section.

## 6. Recent efforts on 1-D thermal stratification modeling

As seen from the modeling efforts reviewed above, system-level codes are unable to give adequate accurate predictions of the thermal stratification phenomenon, while the CFD calculations of the interested components are too expensive. Therefore, some recent efforts have been made to develop advanced 1-D models for thermal stratification. With more validations, these models will be implemented into the system-level codes such that they can facilitate fast calculation for the whole system. After the system-level codes are coupled with CFD codes for more precise calculations, the estimation of the system-level code will be more correct with the implemented 1-D models. They can therefore decrease the iterations between both codes and reduce the calculation time. This section briefly reviews two latest efforts on this regard, executed at the Kansas State University by Wilson and Bindra (2018) and the Virginia Commonwealth University Lu et al. (2019 & 2020), respectively.

### 6.1. The work of Wilson and Bindra

Wilson and Bindra (2018) developed a 1-D scalar transport model to predict the thermal stratification in the upper plena of SFRs under different postulated transients. The axial 1-D model was employed to calculate the centerline temperature of the geometry, and was developed based on the advection-diffusion equation which can be expressed as:

$$\frac{\partial T}{\partial t} = \frac{\partial}{\partial z} \left( \alpha \frac{\partial T}{\partial z} \right) - \frac{\partial}{\partial z} (uT) \quad (1)$$

where  $T$  is the centerline temperature,  $u$  is the jet velocity, and  $\alpha$  is the diffusion coefficient. By assuming the flow to be incompressible and the diffusion coefficient to be axial independent, Eq. (2) was obtained as

$$\frac{\partial T}{\partial t} = \alpha \frac{\partial^2 T}{\partial z^2} - u \frac{\partial T}{\partial z} \quad (2)$$

Because the heat transfer would be enhanced by the turbulence, the diffusion coefficient  $\alpha$  would be larger than the static diffusion coefficient  $\alpha_s$ . The empirical correlation between  $\alpha$  and  $\alpha_s$  developed by Shih et al. (2005) using direct numerical simulations (DNS) was employed. Three mixing regimes were defined according to the ratio of the turbulent Reynolds number  $Re_t$  to the Richardson number  $Ri$ , and the empirical correlations in each mixing regime are summarized in Table 5.

In order to determine the mixing regime of different flow conditions, Wilson and Bindra calculated the jet turbulence Reynolds number by using the definition of Jones and Launder (1973):

$$Re_t = \frac{\rho k^2}{\mu \epsilon}, \quad (3)$$

where  $k$  is the turbulent kinetic energy, and  $\epsilon$  is its dissipation rate. These two turbulence parameters could be estimated by using the

**Table 5**

Correlations between  $\alpha$  and  $\alpha_s$  (Shih et al., 2005).

Regime	$\frac{Re_t}{Ri}$	$\alpha$
Molecular	$\frac{Re_t}{Ri} < 150$	$\alpha_s$
Transitional	$150 < \frac{Re_t}{Ri} < 1000$	$0.015 \alpha_s \frac{Re_t}{Ri}$
Energetic	$1000 < \frac{Re_t}{Ri}$	$0.015 \alpha_s \left( \frac{Re_t}{Ri} \right)^{0.5}$

approximations made by Lai et al. (1986):

$$k = 0.01 U_{jet}^2 \quad (4)$$

$$\varepsilon = \frac{2k^{3/2}}{d_{jet}}, \quad (5)$$

where  $U_{jet}$  is the entering velocity of the jets, and  $d_{jet}$  is the diameter of the inlets of the jets. The jet Richardson number was defined as

$$Ri_{jet} = \frac{(\rho_{jet} - \rho_{amb}) g d_{jet}}{\rho_{amb} U_{jet}^2}, \quad (6)$$

where  $\rho_{jet}$  and  $\rho_{amb}$  are the mass densities of the jet and the ambient fluid, respectively. The authors discretized the 1-D scalar transport equation by using an upwind scheme for the temporal derivative, a second order central difference scheme for the second order spatial derivative, and a third order backward difference scheme for the first order spatial derivative. The discretized form of Eq. (2) was then expressed as

$$\frac{T_i^{n+1} - T_i^n}{\Delta t} = \alpha_i^n \frac{T_{i+1}^n - 2T_i^n + T_{i-1}^n}{\Delta z^2} - u_i \frac{2T_{i+1}^n + 3T_i^n - 6T_{i-1}^n + T_{i-2}^n}{6\Delta z}, \quad (7)$$

where the superscript  $n$  specifies the time step, and the subscript  $i$  specifies the axial node. The authors applied the Dirichlet boundary condition at the inlet to represent the condition where a jet with a constant temperature enters the system, and the Neumann boundary condition at the outlet to represent an insulated condition. The performance of the 1-D transport model was evaluated by comparing the 1-D predictions with the CFD calculations. A cylindrical pool with a height of 1 m and a diameter of 0.2 m was used during the verification process as a simplified geometric representation of an upper plenum in an SFR. The transients considered consisted of cold jets of 50 °C entering from the bottom of the plenum filled with fluid of 200 °C. The mass flow rate of the impinging sodium jets was varied such that all the three mixing regimes were covered. Comparisons of the 1-D prediction with the centerline temperature calculated with the CFD model are shown in Figs. 12–14 for each of the mixing regimes (Wilson and Bindra, 2018).

In the energetic mixing regime, the 1-D model was unable to predict

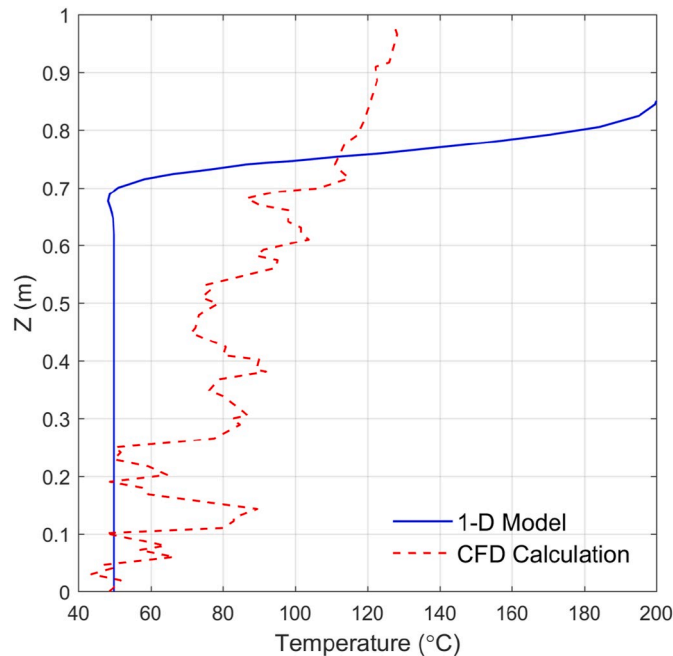


Fig. 12. Axial temperature profile comparison in the energetic regime [ $Re_\tau/Ri = 1.8 \times 10^5$  at  $t = 20$  s] (Wilson and Bindra, 2018).

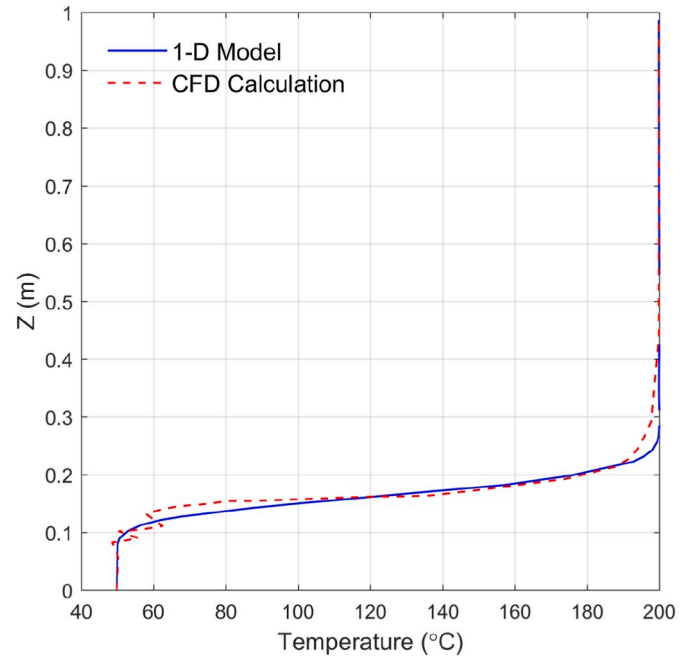


Fig. 13. Axial temperature profile comparison in the transitional regime [ $Re_\tau/Ri = 632$  at  $t = 30$  s] (Wilson and Bindra, 2018).

the temperature profile due to the 3-D nature of the turbulent flow in the plenum caused by the impinging jets with high energy. The 1-D scalar transport model showed reasonable comparison with the CFD calculation within the molecular and transitional mixing regimes, and showed promise to be integrated into the systems-level codes. However, the 1-D model developed by Wilson and Bindra could only predict the coolant temperature along the centerline of the upper plenum, and would therefore be hard to be applied to the cases where the center of the geometry is occupied by the in-vessel components. Moreover, the temperature along the centerline of the upper plenum is different from the temperature of the ambient fluid in the upper plenum, while the latter is

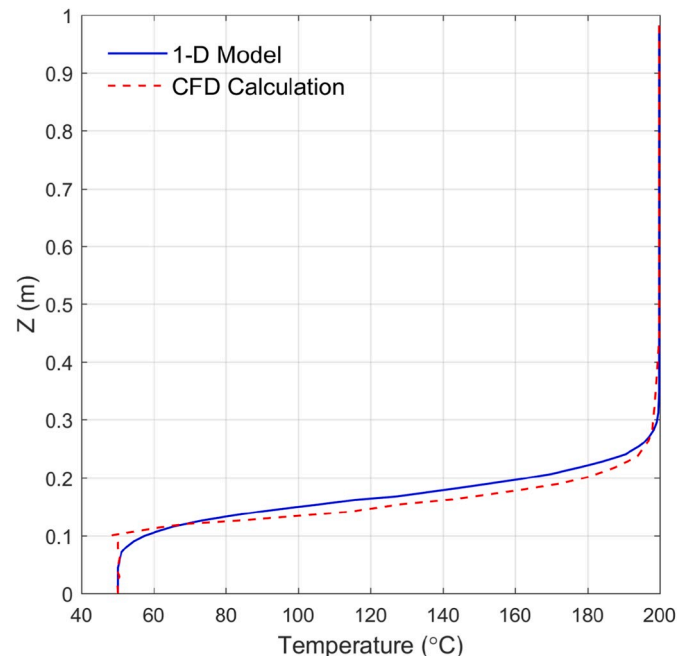


Fig. 14. Axial temperature profile comparison in the molecular regime [ $Re_\tau/Ri = 82$  at  $t = 60$  s] (Wilson and Bindra, 2018).

the one that physically contacts the reactor vessel and the in-vessel components.

## 6.2. The work of Lu et al.

Lu et al. (2019 & 2020) focused on the axial 1-D modeling of the ambient fluid in the upper plenum of an SFR by considering the impinging jet as a heat source of the ambient fluid. Their model was built based on the governing equations developed in the work of Peterson (1994), corresponding to the conservation of mass, momentum, and energy, respectively:

$$A_{amb} \frac{\partial \rho_{amb}}{\partial t} + \frac{\partial(\rho_{amb} Q_{amb})}{\partial z} = \sum_{n=1}^{N_{jet}} \rho_n \dot{Q}_n \quad (8)$$

$$\frac{\partial P_{amb}}{\partial z} = -\rho_{amb} g \quad (9)$$

$$A_{amb} \frac{\partial(\rho_{amb} h_{amb})}{\partial t} + \frac{\partial(\rho_{amb} h_{amb} Q_{amb})}{\partial z} - A_{amb} \frac{\partial}{\partial z} \left( k_{amb} \frac{\partial T_{amb}}{\partial z} \right) = \sum_{n=1}^{N_{jet}} \rho_n h_n \dot{Q}_n, \quad (10)$$

where  $\rho_{amb}$ ,  $h_{amb}$ ,  $k_{amb}$ ,  $A_{amb}$ , and  $T_{amb}$  are respectively the mass density, enthalpy, thermal conductivity, surface area, and temperature of the ambient fluid.  $\rho_n$ ,  $Q_n$ , and  $h_n$  are respectively the mass density, linear volumetric dispersion rate, and the enthalpy of the  $n^{th}$  impinging jet.  $N_{jet}$  is the number of the impinging jets. By combining the mass conservation equation into the energy conservation equation, and assuming small temperature dependency of the sodium heat capacity, Eq. (11) can be obtained, which would be solved for the ambient temperature profile:

$$\rho_{amb} c_p \frac{\partial T_{amb}}{\partial t} + \rho_{amb} c_p u_z \frac{\partial T_{amb}}{\partial z} - \frac{\partial}{\partial z} \left( k_{amb} \frac{\partial T_{amb}}{\partial z} \right) = \frac{N_{jet}}{A_{amb}} c_{p,jet} \rho_{jet} \dot{Q}_{jet} (T_{jet} - T_{sf}) \quad (11)$$

The total linear jet dispersion rate  $\dot{Q}_{jet}$  was the only parameter that needed to be calculated through additional closure equations, and the horizontal surface area averaged velocity was defined as

$$u_z = \frac{Q_{amb}}{A_{amb}} = \frac{\sum_{n=1}^{N_{jet}} \int \dot{Q}_n dz}{A_{amb}} \quad (12)$$

Similar to the work of Wilson and Bindra (2018), the empirical correlation developed by Shih et al. (2005) was employed to take the enhancement of the thermal conductivity due to turbulence into consideration. Instead of the Richardson number of jets, that of the ambient fluid was considered:

$$Ri_{amb} = \frac{g}{\rho_{amb}} \frac{\partial \rho_{amb} / \partial z}{(\partial u_z / \partial z)^2} \quad (13)$$

By assuming that the impinging jets uniformly dispersed in the ambient flow within a length of  $L_{jet}$ , the following approximations were made:

**Table 6**  
Test conditions of the experiments (Lu et al., 2020).

Test No.	Inlet T (°C)	Initial T (°C)	Flow rate (gpm)	Flow rate (L/s)	
1	200	250	6	0.38	With UIS
2	200	250	10	0.63	
3	200	225	10	0.63	
4	200	300	1.5	0.09	Without UIS
5	200	250	3	0.19	
6	200	300	3	0.19	
7	200	250	10	0.63	
8	200	300	10	0.63	

$$\partial \rho_{amb} / \partial z = (\rho_{jet} - \rho_{amb}) / L_{jet} \quad (14)$$

$$\partial u_z / \partial z = \frac{Q_{jet}}{A_{amb}} / L_{jet}. \quad (15)$$

Lu et al. found that the ambient fluid was classed under the molecular regime in all the experimental settings that they considered, as shown in Table 6, which implied that the impinging jets did not introduce significant turbulence to enhance the heat transfer in the ambient fluid in their experiments.

The authors discretized the 1-D model by using the semi-implicit approach for the temporal derivative, a first order upwind scheme for the first order spatial derivative, and a second order central difference scheme for the second order spatial derivative. The discretized form of Eq. (11) is then expressed as

$$\begin{aligned} & \rho_i^n c_{p,i} \frac{T_i^{n+1} - T_i^n}{\Delta t_n} + \rho_i^n c_{p,i} \bar{u}_{z,i}^n \frac{T_i^{n+1} - T_{i-1}^{n+1}}{\Delta z_i} - \frac{2}{\Delta z_i} k_i^n \left[ \frac{T_{i+1}^{n+1} - T_i^{n+1}}{\Delta z_{i+1} + \Delta z_i} - \frac{T_i^{n+1} - T_{i-1}^{n+1}}{\Delta z_i + \Delta z_{i-1}} \right] \\ & = \frac{N_{jet}}{A_{sf}} c_{p,jet} \rho_{jet} \dot{Q}_{jet,i} (T_{jet} - T_i^n) \end{aligned} \quad (16)$$

where the superscript  $n$  specifies the time step, and the subscript  $i$  specifies the axial node. The Neumann boundary condition was used at both the inlet and the outlet to represent an insulated condition. Similar to the work of (Wilson and Bindra, 2018), only the test conditions where cooler jets entering hotter ambient fluid were considered. Because the center of the geometry may be occupied by the in-vessel components, two subcases were further considered in the work of (Lu et al., 2020). In the first subcase, in-vessel components are located close to the inlet of the jet, and the impinging jets will not be able to rise above the in-vessel components before dispersing in the ambient fluid. In tests No. 1–3, an UIS was installed in the tank above the inlets to simulate the in-vessel components in the upper plenum. In the second subcase, no in-vessel components are presented in the plenum, and the impinging jets could reach a higher height. The tests No. 4–8 shown in Table 6 were performed corresponding to this subcase.

In the first subcase, the jet length  $L_{jet}$  was considered to be the distance between the bottom of the UIS and the jet inlet surface, which was about 5 cm in the experiments. The impinging sodium was assumed to be evenly dispersed in the ambient fluid within the jet length:

$$\dot{Q}_{jet} = Q_{jet} / N_{jet} L_{jet} \quad (17)$$

The performance of the 1-D model was evaluated by comparing the 1-D calculations with both the experimental data and the CFD calculations. Fig. 15 shows the temperature of the ambient fluid predicted by the 1-D model at different axial locations as a function of the elapsed

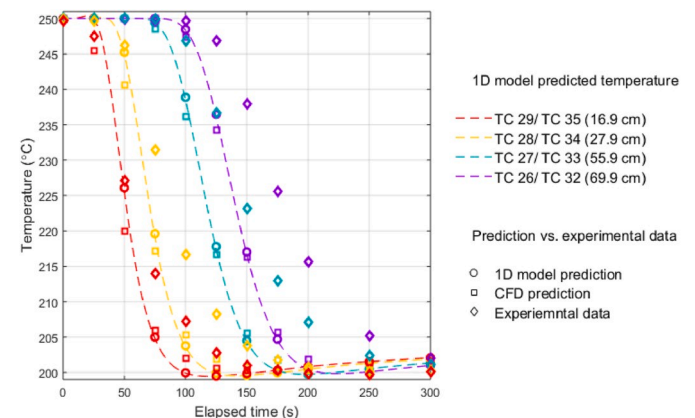


**Fig. 15.** Comparison of the predicted temperature with experimental data at different elapsed time for experiment No. 1 (Lu et al., 2020).

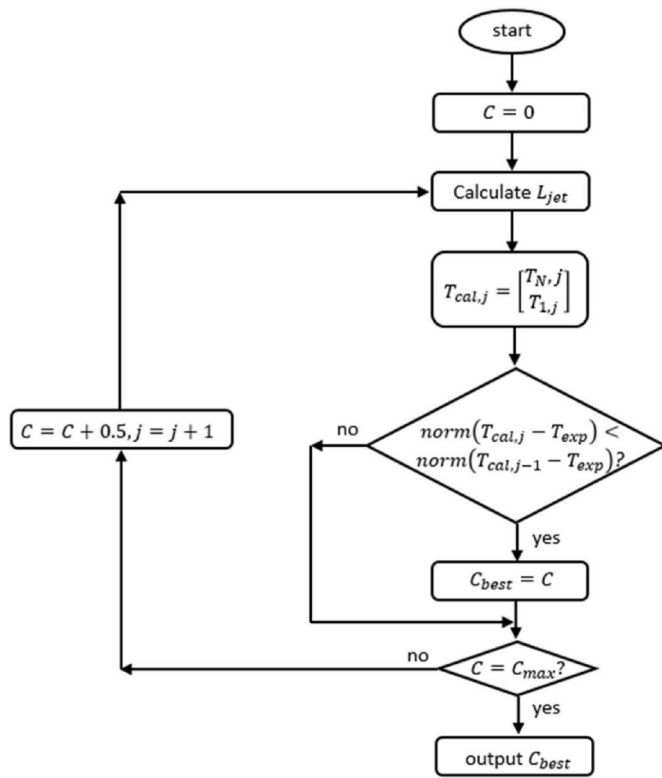


Fig. 16. Diagram of the training process (Lu et al., 2020).

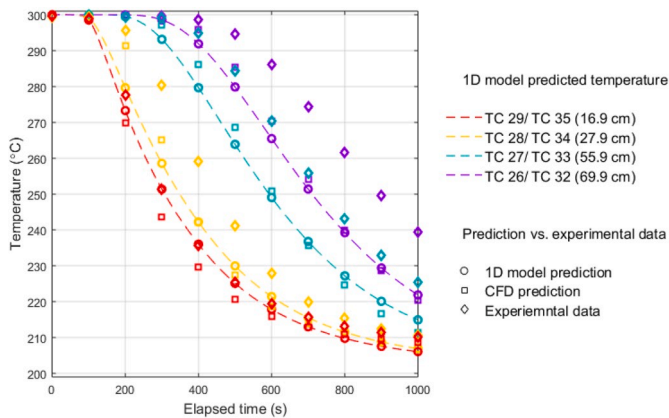


Fig. 17. Comparison of the predicted temperature with experimental data at different elapsed time for experiment #4 (Lu et al., 2020).

time for test No. 1, in comparisons with both the CFD predictions and the experimental data.

In the second subcase, when there was no UIS installed in the tank, the impinging jets could rise without hitting the in-vessel components. Lu et al. analyzed the forces applied to the impinging jet, and calculated the jet length  $L_{jet}$  by integrating the jet velocity over time with:

$$dv_{jet} = - \left( C \frac{v_{jet}^2 \rho_{amb} + \rho_{jet} - \rho_{amb}}{\rho_{jet}} \right) dt, \quad (18)$$

where  $C$  was a coefficient related to the drag force, which was obtained through a data-driven training process which found the coefficient  $C$  that best fitted the experimental data, as shown in Fig. 16. The experimental setting No. 5 and No. 6 were used to train the 1-D model, and the data measured in experimental settings No. 4, No. 7 and No. 8 were used for the validation process. The best fitting coefficient  $C$  was found to be

4.3. Fig. 17 shows the temperature of the ambient fluid predicted by the 1-D model at different axial locations as a function of the elapsed time for test No. 4, in comparison with both the CFD predictions and the experimental data.

In both subcases, the 1-D model developed by Lu et al. showed very good comparisons with both the experimental data and the CFD calculations at lower axial locations. However, despite the similar performance showed by the 1-D model with that of the CFD model, non-negligible discrepancies between the 1-D prediction and the measured data were observed at higher axial locations.

## 7. Future perspective

According to the status review of the development of the thermal stratification modelings, several aspects on the future development of the thermal stratification can be envisioned.

Machine learning methods have been under fast development during the past few years, and could help with the process of developing more cost-effective models for thermal mixing and stratification. The data-driven training process used by Lu et al. (2020) could be considered as an application of the machine learning methods to some extent. Because of the discrepancies observed between the 1-D prediction and the experimental data, the research team is currently considering to improve their 1-D model by adopting less assumptions and approximations, including those used to calculate the linear jets dispersion rate. Instead of assuming a uniform jet dispersion rate and using a simplified model to predict the jet length, the team is planning to find the profiles of the jet dispersion rate as a function of time that provide the best fit with experimental data by using machine learning methods. Furthermore, correlations between the jets dispersion rate profile and the related non-dimensional numbers can be developed and improved via a data-driven technique.

Reduced order modeling (ROM), also known as model reduction, is another possible direction to efficiently model complexing 3-D phenomena such as mixing and thermal stratification. The basic idea in most ROM approaches is to use a relatively small number of solutions generated by a high-fidelity model to construct a computationally tractable model. A successful ROM must be predictive across the design or parameter space of interest (Barone et al., 2009). The System Analysis Module (SAM) is an advanced and modern system analysis tool being developed at ANL (Hu, 2017a). SAM aims for advances in physical modeling, numerical methods, and software engineering to enhance its user experience and usability for reactor transient analyses. A reduced order three-dimensional module is currently under development to enable SAM for thermal mixing and stratification modeling in large enclosures of reactor systems during transients (Hu, 2017b). An overview of the ROM model employed in SAM is provided by Hu (2017b), including the governing equations and closure models, stabilization scheme, numerical discretization schemes, and solution methods. The V&V efforts of the developed ROM model was also included in the work of Hu (2017b), against experimental data of a lid-driven cavity flow and a natural convection inside a cavity.

## 8. Conclusions

Thermal mixing and stratification phenomena play crucial roles in the safety of advanced reactor systems with large fluid volume enclosures, especially the pool-type SFRs. Two modeling methodologies are generally observed to handle the fluid mixing and thermal stratification phenomena that may be encountered in the plena of the SFRs: the traditional system-level approaches and 3-D CFD methods.

The system-level codes use 0-D or 1-D models for the prediction of the thermal stratification phenomenon. They are fast-running, but can only provide approximated solutions for simple conditions of thermal stratification due to the highly simplified and conservative models employed. The CFD methods, on the other hand, can provide high-

resolution calculations to model thermal stratification. However, due to the fine grids required, the CFD calculations are computational expensive and time consuming. Partly due to the prohibitive computational expense associated with the stand-alone CFD models, coupling schemes between the system-level methods and the CFD methods are often considered, particularly when the whole plant transient calculations are needed for reactor safety analyses. In the coupling method, regions of 3-D interest are modeled by the CFD codes, while the rest of the reactor circuit is modeled by the system-level codes. Feedbacks are provided mutually between system-level codes and the CFD codes. However, because the intensive CFD calculations are more or less involved, most of the coupled calculations are still computational expensive.

Some recent attempts have been made to develop improved 1-D models for thermal stratification. With more validations, these models will be implemented into the system-level codes such that they can be used to perform fast whole plant calculations with adequate precision. Based on the status review, new research directions on the development in the modeling of thermal stratification are envisioned, including increasing the accuracy of the 1-D models through machine learning methods, and decreasing the computational expense of the CFD models through ROM.

## Acknowledgement

The work was partially supported by the U.S. Department of Energy Nuclear Energy University Programs (DOE-NEUP) with the Project ID: 16–10268. The experimental data and CFD simulation results presented in Section 6.2 were provided by the project collaborators from University of Wisconsin-Madison and Massachusetts Institute of Technology, respectively.

## References

- Azarian, M., et al., 1990. Sodium thermal hydraulics in the pool LMFBR primary vessel. *Nucl. Eng. Des.* 124, 417–430.
- Barone, M.F., Kalashnikova, I., Brake, M.R., Segalman, D.J., 2009. Reduced Order Modeling of Fluid/structure Interaction. SAND2009-7189.
- Bandini, G., et al., 2015. Assessment of systems codes and their coupling with CFD codes in thermal-hydraulic applications to innovative reactors. *Nucl. Eng. Des.* 281, 22–38.
- Chang, W.P., Kwon, Y.M., Lee, Y.B., Hahn, D., 2002. Model development for analysis of the Korea advanced liquid metal reactor. *Nucl. Eng. Des.* 217, 63–80.
- Choi, C., Ha, K., 2016. Performance test of MARS-LMR code with benchmark analysis of EBR-II SHRT-17. *Ann. Nucl. Energy* 94, 376–391.
- Choi, S.-K., Lee, T.-H., Kim, Y.-I., Hahn, D., 2013. Numerical analysis of thermal stratification in the upper plenum of the MONJU fast reactor. *Nucl. Eng. Technol.* 45 (2), 191–202.
- Doi, Y., Muramatsu, T., 1997. Numerical analysis of thermal of thermal stratification phenomena in upper plenum of fast breeder reactor. In: *Proc. 8th International Topical Meeting on Nuclear Reactor Thermal-Hydraulics*, 3, pp. 1696–1703.
- Fanning, T., Thomas, J., 2010. *Advances in Coupled Safety Modeling Using Systems Analysis and High-Fidelity Methods*. Argonne National Laboratory (ANL) ANL-GENIV-134.
- Fanning, T., Thomas, J., Sumner, T., Brunett, A., 2015. Recent developments for the SAS4A/SASSYS-1 safety analysis code. In: *Proceedings of NURETH-16*, Chicago, IL, August 30–September 4.
- Fanning, T.H., et al., 2017. The SAS4A/SASSYS-1 Safety Analysis Code System, ANL/NE-16/19. Nuclear Engineering Division, Argonne National Laboratory (ANL).
- Gamble, R.E., et al., 2001. Pressure suppression pool mixing in passive advanced BWR plants. *Nucl. Eng. Des.* 204, 321–336.
- Geffraye, G., et al., 2009. CATHARE 2 v2.5.2: a single version for various applications. In: *Proceedings of NURETH-13*, Kanazawa, Ishikawa, Japan, Sep. 27 – Oct. 2.
- Hu, R., 2017a. SAM Theory Manual. Argonne National Laboratory (ANL). ANL/NE-17/4.
- Hu, R., 2017b. Development of a reduced order three-dimensional flow model for thermal mixing and stratification simulation during Reactor Transients. In: *The 17th International Topical Meeting on Nuclear Reactor Thermal Hydraulics (NURETH-17)*, Xi'an, China, September 3–8.
- IAEA, 2000. Heat Transport and Afterheat Removal for Gas Cooled Reactors under Accident Conditions. IAEA-TECDOC-1163.
- IAEA, 2009. Passive Safety Systems and Natural Circulation in Water Cooled Nuclear Power Plants. IAEA-TECDOC-1624.
- Ieda, Y., Maekawa, I., Muramatsu, T., Nakanishi, S., 1990. Experimental and analytical studies of the thermal stratification phenomenon in the outlet plenum of fast breeder reactors. *Nucl. Eng. Des.* 120 (2–3), 403–414.
- Idaho National Laboratory, 2015. RELAP5-3D Code Manual Volume I: Code Structure, System Models and Solution Methods Revision 4.3 INL/MIS-15-36723.
- Information Systems Laboratories, 2003. RELAP5/MOD3.3 Code Manual, Vol. 1: Code Structure, System Models, and Solution Methods. NUREG/CR-5535/Rev P3-Vol I.
- Jeong, H.Y., Ha, K.-S., Choi, C.-W., Park, M.-G., 2015. Analysis of Phenix End-of-Life asymmetry test with multi-dimensional pool modeling of MARS-LMR code. *Ann. Nucl. Energy* 75, 443–451.
- Jones, W.P., Launder, B.E., 1973. The calculation of low-Reynolds-number phenomena with a two-equation model of turbulence. *Int. J. Heat Mass Tran.* 16, 1119–1130.
- Kamide, H., Kobayashi, J., Ono, A., Kimura, N., Watanabe, O., 2011. Sodium experiment on fully natural circulation systems for decay heat removal in Japan sodium-cooling fast reactor. In: *Proceedings of NURETH*, vol. 14. Toronto, Canada. No.179.
- Kimura, N., Miyakoshi, H., Kamide, H., 2010. Experimental study on thermal stratification in a reactor vessel of innovative sodium-cooled fast reactor - mitigation approach of temperature gradient across stratification interface-. *J. Nucl. Sci. Technol.* 47 (9), 829–838.
- Kwon, Y.M., et al., 2000. SSC-K Code User's Manual (Rev.0). Korea Atomic Energy Research and Institute. KAERI/TR-1619/2000.
- Lai, K.Y.M., Salcudean, M., Tanaka, S., Guthrie, R.L.L., 1986. Mathematical modeling of flows in large tundish systems in steelmaking. *Metall. Trans. B* 17B, 449–459.
- Lee, Y.B., et al., 2000. Development of Two-Dimensional Hot Pool Model. Korea Atomic Energy Research and Institute. KAERI/TR-1566/2000.
- Lerchel, G., Austregesilo, H., 2006. ATHLET Mod 2.1 Cycle A, User's Manual, GRS-P-1, vol. 1. Rev. 4. GRS, Germany.
- Lu, C., et al., 2019. Thermal stratification analysis for sodium-cooled fast reactors: development of the 1-D model for the system codes. *Trans. Am. Nucl. Soc.* 121, 1703–1706.
- Lu, C., et al., 2020. An Efficient 1-D Thermal Stratification Model for Pool-type Sodium-cooled Fast Reactors. *Nuclear Technology* (Accepted).
- Ma, W.M., Karbojian, A., Sehgal, B.R., 2007. Experimental study on natural circulation and its stability in a heavy liquid metal loop. *Nucl. Eng. Des.* 237, 1838–1847.
- Maekawa, I., Ninokata, H., Bottoni, M., et al., 1991. Assessment and implementation of second-order schemes for advection terms in general-purpose 3D thermohydraulics computer codes. In: *7th Int. Conf. Numerical Methods in Thermal Problems*, Stanford, CA, USA, Jul. 8–12.
- Mochizuki, H., Yao, H., 2014. Analysis of thermal stratification in the upper plenum of the “Monju” reactor. *Nucl. Eng. Des.* 270, 48–59.
- Morgan, S., et al., 2018. Thermal stratification modeling for sodium-cooled fast reactors: a status update. In: *Proceedings of the 26th International Conference on Nuclear Engineering (ICONE-26)*, London, England, July 22–26.
- Moriya, S., Tanaka, N., Katano, N., Wada, A., 1987. Effects of Reynolds number and Richardson number on thermal stratification in hot plenum. *Nucl. Eng. Des.* 99, 441–451.
- Munkhzul, E., Thomas, J., 2014. CFD simulations of the effects of thermal stratification on the start of natural circulation during SFR transients. In: *International Congress on Advances in Nuclear Power Plants (ICAPP)*.
- Muramatsu, T., Ninokata, H., 1994. Investigation of turbulence modelling in thermal stratification analysis. *Nucl. Eng. Des.* 150 (1), 81–93.
- Narcisi, V., Giannetti, F., Caruso, G., 2019. Investigation on RELAP5-3D© capability to predict thermal stratification in liquid metal pool-type system and comparison with experimental data. *Nucl. Eng. Des.* 352 (110152).
- Niu, F., et al., 2007. Investigation of mixed convection in a large rectangular enclosure. *Nucl. Eng. Des.* 237, 1025–1032.
- Note SYFRA 91151, 1993. Programme DYN2B – Note générale de présentation.
- Ohira, H., et al., 2013. Benchmark analyses of sodium natural convection in the upper plenum of the MONJU reactor vessel. In: *International Conference on Fast Reactors and Related Fuel Cycles: Safe Technologies and Sustainable Scenarios (FR13)*, IAEA-CN-199/142.
- Ohno, S., Ohki, H., Sugahara, A., Ohshima, H., 2011. Validation of a computational simulation method for evaluating thermal stratification in the reactor vessel upper plenum of fast reactors. *J. Nucl. Sci. Technol.* 48 (2), 205–214.
- Oyama, K., et al., 2016. Development of natural circulation analysis methods for a sodium cooled fast reactor. *J. Nucl. Sci. Technol.* 53 (3), 353–370.
- Peterson, P.F., 1994. Scaling and analysis of mixing in large stratified volumes. *Int. J. Heat Mass Tran.* 37, 97–106.
- Pialla, D., et al., 2015. Overview of the system alone and system/CFD coupled calculations of the PHENIX Natural Circulation Test within the THINS project. *Nucl. Eng. Des.* 290, 78–86.
- Schneider, J., et al., 2019. Thermal stratification in a pool-type geometry. In: *The 19th International Topical Meeting on Nuclear Reactor Thermal Hydraulics (NURETH-19)*, Portland, OR, August 18–23.
- Sakamoto, T., Shibahara, M., Takata, T., Yamaguchi, A., 2010. Numerical study of three dimensional thermal hydraulics effect on thermal stratification phenomena in upper plenum of MONJU. In: *Proc. Korea-Japan Symposium on Nuclear Thermal Hydraulics and Safety (NTHAS-7)*.
- Shibahara, M., Takata, T., Yamaguchi, A., 2013. Numerical study on thermal stratification phenomena in upper plenum of LMFBR “monju”. *Nucl. Eng. Des.* 258, 226–234.
- Shih, L.H., Koseff, J.R., Ivey, G.N., Ferziger, J.H., 2005. Parameterization of turbulent fluxes and scales using homogeneous sheared stably stratified turbulence simulations. *J. Fluid Mech.* 525, 193–214.
- Sofu, T., 2012. Parametric Analysis of Thermal Stratification during the MONJU Turbine Trip Test. *Tech. Rep.*, vol. 555. American Nuclear Society, North Kensington Avenue, La Grange Park, IL 60526.
- Sumner, T., Moiseyev, A., 2015. Simulation of the EBR-II Tests SHRT-17 and SHRT-45R. *NURETH-16*, Chicago, IL, August 30–September 4, 2015.
- Tanaka, N., Moriya, S., Ushijima, S., Koga, T., Eguchi, Y., 1990. Prediction method for thermal stratification in a reactor vessel. *Nucl. Eng. Des.* 120 (2–3), 395–402.

- Tenchine, D., et al., 2012. Status of TRIO\_U code for sodium cooled fast reactors. Nucl. Eng. Des. 242, 307–315.
- Thomas, J., Fanning, T., Vilim, R., Briggs, L., 2012. Validation of the Integration of CFD and SAS4A/SASSY-1: Analysis of EBR-II Shutdown Heat Removal Test 17, vol. 555. American Nuclear Society, North Kensington Avenue, La Grange Park, IL 60526 (United States), 2012.
- U. S. Nuclear Regulatory Commission, 2001. TRAC-M/FORTRAN 90 (Version 3.0) Theory Manual, NUREG/CR-6724.
- U. S. Nuclear Regulatory Commission, 2005. MELCOR Computer Code Manuals, NUREG/CR-6119, vol. 2, Rev. 3, SAND 2005-5713.
- Vidil, R., Grand, D., Leroux, F., 1988. Interaction of recirculation and stable stratification in a rectangular cavity filled with sodium. Nucl. Eng. Des. 105 (3), 321–332.
- Wang, S., Zhang, D., Song, P., Zhang, Y., Wang, M., Wu, Y., Qiu, S., 2018. Validation of a methodology for thermal stratification analysis in sodium-cooled fast reactors. Int. J. Energy Res. 42, 3803–3822.
- Ward, B., Wiley, A., Wilson, G., Bindra, H., 2018. Scaling of thermal stratification or mixing in outlet plena of SFRs. Ann. Nucl. Energy 112, 431–438.
- Ward, B., Clark, J., Bindra, H., 2019. Thermal stratification in liquid metal pools under influence of penetrating colder jets. Exp. Therm. Fluid Sci. 103, 118–125.
- Watanabe, O., et al., 2015. Development of an evaluation methodology for the natural circulation decay heat removal system in a sodium cooled fast reactor. J. Nucl. Sci. Technol. 52 (9), 1102–1121.
- Wilson, G., Bindra, H., 2018. Thermal Stratification and Mixing in SFR Plena Using a One-Dimensional Scalar Transport Model. ATH 2018, Orlando, Florida. November 11–15.
- Yamada, F., Fukano, Y., Nishi, H., Konomura, M., 2014. Development of natural circulation analytical model in Super-COPD code and evaluation of core cooling capability in Monju during a Station Blackout. Nucl. Technol. 188 (3), 292–321.
- Yue, N., Ma, Z., Cai, R., Hu, B., Su, G.H., Qiu, S., 2015. Thermal-hydraulic analysis of EBR-II shutdown heat removal tests SHRT-17 and SHRT-45R. Prog. Nucl. Energy 85, 682–693.
- Zhao, H., Peterson, P.F., 2007. One-dimensional Analysis of Thermal Stratification in AHTR and SFR Coolant Pools. INL/CON-06-12026.
- Zhao, H., Peterson, P.F., 2009. One-dimensional analysis of thermal stratification in AHTR coolant pool. Nucl. Eng. Technol. 41 (7), 953–968.
- Zhao, H., Peterson, P.F., 2010. An overview of modeling methods for thermal mixing and stratification in large enclosures for reactor safety analysis. In: The 8th International Topical Meeting on Nuclear Thermal-Hydraulics, Operation and Safety (NUTHOS-8), Shanghai, China, October 10–14, 2010.
- Zhou, C., Huber, K., Cheng, X., 2013. Validation of the modified ATHLET code with the natural convection test of the PHENIX reactor. Ann. Nucl. Energy 59, 31–46.
- Zwijnsen, K., Dovizio, D., Moreau, V., Roelofs, F., 2019. CFD modelling of the CIRCE facility. Nucl. Eng. Des. 353, 110277.